# Spatial, temporal and evolutionary insight into seasonal epidemic Influenza A virus strains near the equatorial line: The case of Ecuador

Alfredo Bruno [a,d], Natalia Goñi [b], Juan Cristina [c,*]

[a] Centro de Referencia Nacional de Influenza y otros Virus Respiratorios, Instituto Nacional de Investigación en Salud Pública, Guayaquil, Ecuador
[b] Departamento de Laboratorios de Salud Pública, Ministerio de Salud Pública, Centro Nacional de Referencia de Influenza, Montevideo, Uruguay
[c] Laboratorio de Virología Molecular, Centro de Investigaciones Nucleares, Facultad de Ciencias, Universidad de la República, Iguá 4225, Montevideo 11400, Uruguay
[d] Universidad Agraria del Ecuador, Av. 25 de Julio, Guayaquil 090104, Ecuador

ABSTRACT

To study the spatial and temporal patterns of Influenza A virus (IAV) is essential for an efficient control of the disease caused by IAV and efficient vaccination programs. However, spatiotemporal patterns of spread as well as genetic lineage circulation of IAV on a countrywide scale have not been clearly determined for many tropical regions of the world. In order to gain insight into these matters, the spatial and temporal patterns of IAV in six different geographic regions of Ecuador, from 2011 to 2021, were determined and the timing and magnitude of IAV outbreaks in these localities investigated. The results of these studies revealed that although Ecuador is a South American country situated in the Equator line, its IAV epidemiology resembles that of temperate Northern Hemisphere countries. Phylogenetic analysis of H1N1pdm09 and H3N2 IAV strains isolated in five different localities of Ecuador revealed that provinces in the south of this country have the largest effective population size by comparison with provinces in the north, suggesting that the southern provinces may be acting as a source of IAV. Co-circulation of different H1N1pdm09 and H3N2 genetic lineages was observed in different geographic regions of Ecuador.

## 1. Introduction

Influenza A virus (IAV) is a member of the family *Orthomyxoviridae* and contains eight segments of a single-stranded RNA genome with negative polarity (Neumann et al., 2004). Unlike most pathogens where exposure leads to lasting immunity in the host, IAV has the capacity of evade specific immunity triggered by previous infections. This process is called antigenic drift and is the result of the selective fixation of mutations in the gene encoding the hemagglutinin (HA) protein, the major target for the host immune response. Another process, called antigenic shift, occurs when the virus acquires an HA of a different IAV subtype via reassortment of one or more gene segments. This process is thought to be related to the more devastating Influenza pandemics (Ferguson et al., 2003).

There have been three pandemics in last century: in 1918 (H1N1 subtype), 1957 (H2N2 subtype), and in 1968 (H3N2 subtype). During each of these pandemics, the new virus drove the previous pandemic subtype out of circulation (Wolf et al., 2006). In 1977, the H1N1 subtype reappeared, and has been co-circulating with H3N2 subtype to present

days (Scholtissek et al., 1978). In 2009, the first pandemic of this century, caused by a new H1N1 pdm09 strain started in Mexico and spread to many several other countries around the world (Scalera and Mossad, 2009).

The global surveillance of IAV have provided an opportunity to explore the drivers of global spread of these viruses (Lemey et al., 2014). However, spatiotemporal patterns of spread as well as genetic lineage circulation of IAV on a countrywide scale have not been clearly determined form any tropical regions of the world (Hirve et al., 2016; Azziz et al., 2012; Viboud et al., 2006). A more complete understanding of the evolution of IAV in these regions are much needed in order to a more efficient control of the disease caused by IAV and efficient vaccination programs. In order to gain insight into these matters, we used a ten-year dataset of 4038 typed, subtyped and antigenically characterized seasonal IAV strains circulating in six different geographic regions of Ecuador and investigated the timing and magnitude of IAV outbreaks in these localities. Besides, we isolated, sequenced, and analyzed the complete codes of 120 HA genes of H1N1 pdm09 and H3N2 IAV strains, sampled between 2016 and 2020 isolated in five Ecuadorian locations.

We have found that although Ecuador is a tropical South American country; its epidemiology resembles that of temperate Northern Hemisphere countries.

## 2. Materials and methods

### 2.1. Samples sources

Samples analyzed in these studies were collected from severe acute respiratory infection Ecuadorian surveillance system, in the laboratory of the National Influenza centre; the number of processed samples and Influenza virus positivity per epidemiological week was obtained from the data reported in the WHO Flunet platform; all the genetic sequence were obtained from GISAID platform.

The proposal does not constitute research with human subjects. As a laboratory within the World Health Organization (WHO) Global Influenza Surveillance and Response System (GISRS) for the purposes of global surveillance of Influenza under the WHO Global Influenza Program, neither written inform consents nor explicit ethical approval were sought as this study was only observational and carried out as part of a routine virological surveillance (anonymously, without identification of patients), as established in the terms of reference for WHO National Influenza Centers. In accordance with applicable laws and regulations, no clearance of an Ethics Committee is required in Ecuador for the retrospective analysis of anonymized data collected within routine Influenza surveillance schemes.

### 2.2. Climate data

For each of the six provinces of Ecuador studied, we compiled monthly mean temperature ($°C$), mean relative humidity (%) and mean precipitation (mm) from Climate-Data.org (available at: www.es.climate-data.org).

### 2.3. Statistical analysis

Correlation among variables were established using Pearson product-moment correlation test (Wessa, 2023).

### 2.4. Virus antigenic characterization by hemagglutination inhibition assay

The International Reference Center (CDC, Atlanta) performed the hemagglutination inhibition (HI) tests with a panel of post infection ferret antisera for detailed antigenic characterization and also performed a functional neuraminidase inhibition assay (NI) and/or genetic analysis to assess susceptibility of these viruses to the neuraminidase inhibitors oseltamivir, zanamivir, peramivir and laninamivir.

### 2.5. PCR amplification and sequencing of ha gene from Ecuadorian IAV strains

For molecular detection of Influenza virus, the CDC Protocol for Real-Time RT-PCR (rRT-PCR) for the detection and characterization of Influenza A and Influenza B used for the National Influenza Centers was used using Ambion AgPath-ID™ One-Step RT-PCR Kit enzyme (cat# AM1005).(CDC, 2022a)

RNA was extracted using the QIAamp RNA Viral Minikit from Qiagen.

The primers and probes used for the identification of Influenza types and subtypes are those distributed as part of the support provided by the CDC to the National Influenza Centers and distributed through the International Reagent Resource (IRR) portal.

The IRR kit used for Influenza A and B virus typing was the FR-1701 - CDC Influenza Virus Real-Time RT-PCR Influenza A (H3/H1pdm09) Subtyping Panel (VER 3) (RUO) (Catalog No. FluRUO-15).

The kit used for Influenza Virus H1 and H3 subtyping was the FR-1711 - CDC Influenza Virus Real-Time RT-PCR Influenza A/B Typing Panel (VER 2) (RUO) (Catalog No. FluRUO-14).(CDC, 2022b)

PCR master mix were prepared according to the following: Nuclease-free water: $N$ x 5.0 μl first forward primer (0.8 μM final concentration); $N$ x 0.5 μl; Indirect primer (first reverse primer) (0.8 μM final concentration); $N$ x 0.5 μl Probe (probe) (0.2 μM final concentration); $N$ x 0.5 μl; RT Mix $N$ x 1 μl and 2X PCR Master Mix $N$ x 12.5 μl.

The Roche Light Cycler 480 II thermal cycler was used for the nucleic acid amplification process, using the following amplification conditions:

Reverse Transcription: 50 °C for 30 min. Inactivation of Taq inhibitor 95 °C for 10 min. PCR amplification (45 cycles) 95 °C for 15 s; 55 °C for 30 s * PCR amplification (45 cycles) 95 °C for 15 s; 55 °C for 30 s *Fluorescence (FAM) data were collected during the 55 °C incubation step. Sequencing was carried out by the Centers for Disease Control, Atlanta, USA within the commitments of the Global Influenza Surveillance and Response System for the shipment of periodic samples by the National Influenza Center to the WHO collaborating center. Nucleotide sequences of the Ecuadorian Influenza viruses generated in this study have been deposited in the GISAID database (for accession numbers, strain name, date and place of isolation, see Supplementary Material Table 1).

### 2.6. Epidemiological time series

In order to extract and visualize of temporal parameters from epidemiological time series, we employed EPIPOI (Alonso and McCormick, 2012). This approach to time series analysis permits to study long term trends, seasonality and anomalies (for example, morbidity figures in particularly severe epidemics as compared to those figures expected based on the trend and regular seasonal and inter-annual variance in surrounding years). Moreover, EPIPOI approach also allows all parameters describing the components of time series from different locations to be plotted and analyzed spatially. For instance, it can show if the timing of the annual peak of a disease change along a latitudinal gradient (Alonso and McCormick, 2012).

### 2.7. Phylogenetic analysis

Complete HA gene sequences from H1N1pdm09 and H3N2 isolated in the Equatorial provinces of Guayas, Pichincha, Chimborazo, Cañar and Azuay, isolated between 2016 and 2020, were used throughout these studies. For accession numbers, origin and date of isolation, see Supplementary Material Table 1. Sequences were aligned using MAFFT version 7 program (Katoh et al., 2019).

To reconstruct the evolutionary history of IAV strains circulating in Ecuador, a Bayesian Markov Chain Monte Carlo (MCMC) approach was employed using MASCOT v2.1.2 (Muller et al., 2018) as implemented in the BEAST package v2.5.2 (Bouckaert et al.,2019). MASCOT approach implements a structured coalescent approximation by integrating over all possible migration histories. In contrast with other approximations that treat the movement of one lineage completely independently of all other lineages, this approach explicitly includes information about the location of other lineages and their probability of coalescing when modeling the movement of a lineage. First, the evolutionary model that best fit the sequence datasetwas determined using the W-IQ-TREE program (Trifinopoulos et al., 2016). Bayesian information criterion (BIC), Akaike information criterion (AIC), and the log of the likelihood (LnL) were used to identify the best model. Statistical uncertainty in the data was reflected by the 95% highestprobability density (HPD) values. Results were examined using theTRACER v1.7.2 program (available from http://beast.bio.ed.ac.uk/Tracer). Convergence was assessed by effective sample sizes (ESS) above 200. Maximum clade credibility trees were generatedby means of the use of the Tree Annotator program from the BEASTpackage. This method provides a phylogenetic tree that evaluates each of the sampled posterior trees, giving a tree that summarize the results of a Bayesian phylogeny inference. Visualization of the

phylogenetic trees were done using FigTree v1.4.4 (available at: http://tree.bio.ed.ac.uk/).

## 3. Results

### 3.1. Estimating seasonal parameters

To study the seasonal activity of IAV in Ecuador, time-series analyses were performed using the EPIPOI epidemiological software package (Alonso and McCormick, 2012).

We analyzed the total number of IAV positive cases per month from January 2011 to December 2021, for a total of 4038 cases from six different geographic regions of Ecuador (see Supplementary Material Fig. 1). The periodic annual function (PAF) of the epidemiological time series was obtained after de-trending with a quadratic polynomial and summing up the annual, semi-annual and quarterly harmonics as obtained by Fourier decomposition (see Fig. 1). Interestingly, our time-series analysis reveals a well-defined annual periodicity (seasonality) resembling the seasonality found for northern hemisphere temperate countries, characterized by epidemic peaks in the winter season of that hemisphere. Next, we estimated the timing and amplitude of the annual primary peak from 2011 to 2021 for each Ecuadorian location studied. Timing of the annual primary peak is when the maximum annual intensity of IAV activity is detected, whereas peak amplitude is equivalent to the strength of the epidemic cycle. We analyzed these parameters as a function of latitude of each location. The results of these studies are shown in Fig. 2.

Monthly primary peaks were established in January for all the Ecuadorian regions studied, (see Fig. 2 and Supplementary Material Fig. 1). Monthly secondary peaks were observed during May for localities in the north and center of Ecuador (Pichincha, Imbabura and Chimborazo), while monthly secondary peaks were observed in August and September for provinces in the south, like Guayas and Azuay (see Fig. 2 and Supplementary Material Fig. 1). Then, the amplitude of primary and secondary peaks was calculated (see Table 1). Roughly similar amplitudes were found for primary peaks for all geographic locations studied. In the case of the amplitudes found for secondary peaks, significant differences ($> 30\%$) were found for Guayas provinces by comparison with other provinces studied (see Table 1).

In order to observe if climatic factors may be related to the seasonality observed, mean monthly temperature (°C), precipitation (mm) and humidity (%) were established for all geographic locations studied (see Fig. 3). Primary peak of IAV infections occurs during periods of high precipitation and humidity (see Figs. 2 and 3). Interestingly, significant differences in mean monthly temperatures among Guayas and the rest of the locations studied was found. This is related to the fact that Guayas is situated at sea level with a tropical climate, whereas the rest of the provinces are situated at high altitudes (see also Supplementary Material Fig. 1). Moreover, a significant correlation among mean monthly Influenza cases from 2011 to 2021 and mean monthly temperatures was found for Guayas province (Pearson Cor. = 0.6139, $p < 0.05$). No

correlation among mean monthly Influenza cases and mean monthly temperatures was found for the rest of the provinces studied.

### 3.2. Bayesian coalescent analysis of IAV isolated in Ecuador

In order to reconstruct the evolutionary history of IAV populations circulating in different Ecuadorian localities, a Bayesian MCMC approach was employed (Bouckaertet al., 2019) using complete codes from HA genes from 67 H1N1 pdm09 (isolated from 2016 to 2020), and 56 H3N2 IAV strains (isolated from 2016 to 2019) from five different Ecuadorian locations (for isolates included in these analyses, see Supplementary Material Table 1). The results shown in Table 2 are the outcome of 20 million steps of the MCMC, using the HKY+γ nucleotide model, a relaxed molecular clock and a structured coalescent method using MASCOT (Muller et al., 2018).

Mean estimates indicated that Guayas province has the largest effective population size compared with any other Ecuadorian localities studied for H1N1 pdm09 strains. In the case of H3N2 IAV sub-type, Guayas and Cañar provinces have the largest effective population size by comparison with other provinces included in these analyses (see Table 2).

In order to establish the genetic relations among IAV circulating in Ecuador maximum clade credibility trees were constructed for H1N1 pdm09 and H3N2 IAV strains (see Fig. 4). The results of this studies revealed that different genetic lineages co-circulate in different geographic locations of Ecuador. For instance, at least two different H1N1 pdm09 genetic lineages were observed to co-circulate in 2016 in different provinces of the country (see Fig. 4A). In the case of H3N2 strains, several lineages were found to co-circulate in several provinces in 2017 (see Fig. 4B).

## 4. Discussion

WHO annual Influenza vaccine recommendations are designed to ensure vaccine delivery before the winter-time peak of viral circulation in each hemisphere. However, Influenza seasonal patterns are highly diverse in tropical countries and may be out of phase with the WHO recommendations for their respective hemisphere (Alonso et al., 2015). In fact, previous studies revealed that optimal timing for Influenza vaccination may not correspond to the one expected for their hemisphere in tropical regions of South America (De Mello et al., 2009). In order to gain insight into IAV dynamics in a tropical country as Ecuador, we estimated the seasonal parameters and obtained the periodical time function for IAV epidemics in this country (see Fig. 1). The results of these studies revealed that although Ecuador is a tropical South American country, its epidemiology resembles that of temperate Northern Hemisphere countries, with monthly primary peaks in January (see Figs. 1 and 2).

Moreover, these results suggest that Ecuador is 'out-of-phase' from the recommendations of the use of the Southern hemisphere vaccine and more likely is suitable for receiving the vaccine initially recommended
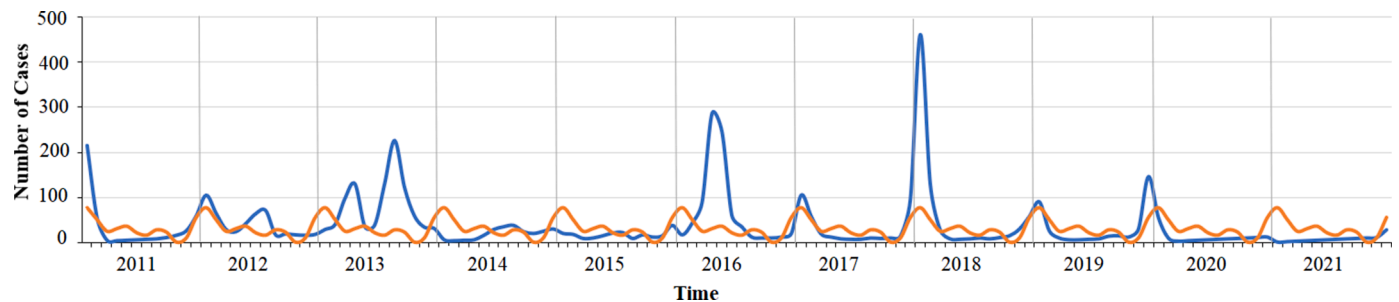


**Fig. 1.** Seasonality of Influenza A in Ecuador (2011–2021). The periodic annual function obtained by summing the 12-monthly,6-monthly and 3-monthly harmonics is shown in orange. The original time series is shown in blue.
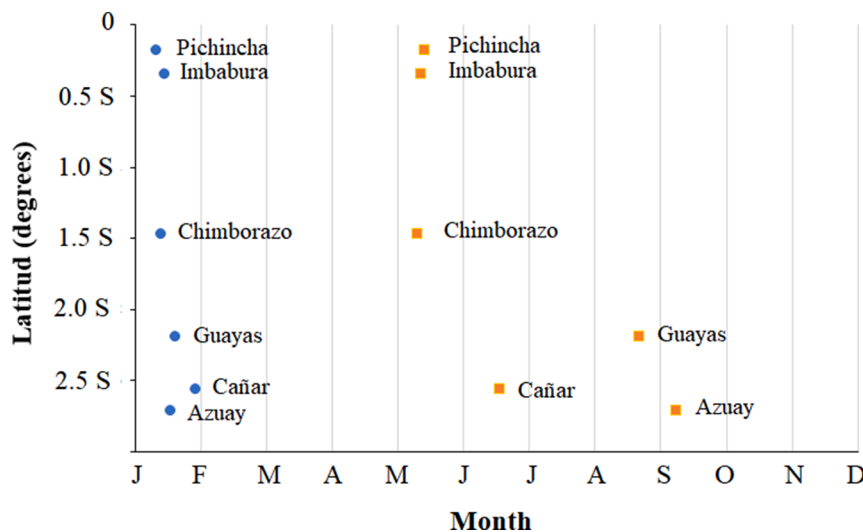
**Fig. 2.** Timing of the monthly primary and secondary peaks of Influenza A in six different Ecuadorian provinces. The timing of the primary and secondary peak against the latitudinal position of each province is shown. Primary peaks are shown by blue circles, while secondary peaks are shown by orange squares.

**Table 1**
Time-series parameters found in the seasonality studies of IAV in Ecuador.

| Series | Latitude Amplitude primary peak (%) | Longitude Amplitude secondary peak (%) | Month primary peak | Month secondary peak |
|---|---|---|---|---|
| Pichincha | 0.1807 S 104.146 | 78.4678 W 63.420 | 1.326 | 5.416 |
| Imbabura | 0.3500 S 95.100 | 78.1167 W 45.658 | 1.453 | 5.366 |
| Chimborazo | 1.4695 S 98.427 | 78.8168 W 45.290 | 1.403 | 5.303 |
| Guayas | 2.1961 S 106.332 | 79.8862 W 80.530 | 1.623 | 8.676 |
| Cañar | 2.5606 S 90.483 | 78.9394 W 51.266 | 1.926 | 6.556 |
| Azuay | 2.7138 S 93.197 | 78.8892 W 12.002 | 1.550 | 9.243 |

for the opposite hemisphere.

The WHO Influenza vaccine committee meet twice a year since 1999 to decide on the antigenic composition of Influenza vaccines for the next Influenza season in each hemisphere (Kitler et al., 2002). In the case of the Northern hemisphere, globally circulating Influenza virus strains are reviewed every February, so that the vaccine can be distributed between September and October, in advance of the winter Influenza season of this hemisphere. Likewise, for the Southern hemisphere, Influenza virus circulation patterns are reviewed each September, so that vaccination can takes place between March and April of the following year. The current six-month delay between the WHO expert recommendations and vaccine availability is due to limitations of the current technology used in the manufacturing process, which represents a severe challenge for vaccine efficacy (Richard et al., 2010). For these reasons, it is important to investigate national patterns of Influenza virus circulation in tropical countries in order to estimate the most appropriate timing for administering the most appropriate Influenza vaccine. The results of these studies revealed that the Northern hemisphere schedule is more appropriate for Ecuador (see Figs. 1 and 2).

Monthly primary peaks revealed a strong correlation with high precipitation and humidity months in all Ecuadorian locations studied (see Figs. 2 and 3). This is in agreement with previous studies suggesting that epidemics in tropical and sub-tropical regions often occur during periods of high humidity (Tamerius et al., 2013). This pattern was also observed in other tropical regions of the world, like Thailand (Suntronwong et al., 2020) or Cote dÍvoire, where rainfall is a good predictor of Influenza activity (Nattia et al., 2016). In the case of Central America, the overall Influenza activity was consistently associated with increased specific humidity in three different tropical countries, but different results were found in the association of temperature and the rainfall, where a positive correlation was found for El Salvador and Panama, but a negative correlation was found for Guatemala (Soebiyanto et al., 2014). This speaks of the need of the characterization of Influenza activity in each particular tropical country.

Guayas province was found to have the larger effective population size for H1N1 pdm09 IAV strains, while Guayas and Cañar were found to have the larger ones in the case of H3N2 IAV population (see Table 2). The results of these studies suggest that provinces in the South of Ecuador may act as a source of Influenza while other provinces may act as a sink (see Table 2 and Supplementary Material Fig. 1). More studies will be needed to address this important issue. Co-circulation of different genetic lineages was observed in both H1N1 pdm09 and H3N2 strains isolated in Ecuador during the same epidemic year (Fig. 4). Moreover, the results of these studies revealed that different genetic lineages co-circulate in different geographic regions of Ecuador at the same time.

## 5. Conclusions

The results of these studies revealed that although Ecuador is a South American country situated in the Equator line, its IAV epidemiology resembles that of temperate Northern Hemisphere countries, with monthly primary peaks in January. These facts revealed that the Northern hemisphere Influenza vaccination schedule is more appropriate for Ecuador. Monthly primary peaks revealed a strong correlation with high precipitation and humidity months in all Ecuadorian locations studied as observed in other tropical regions of the world. Monthly secondary peaks were observed in May for localities in the north and center of Ecuador, while monthly secondary peaks were observed in August and September for provinces in the south. Differences in secondary peak amplitude were observed for Guayas province. Guayas province was found to have the largest effective population size for H1N1 pdm09 IAV strains, while Guayas and Cañar were found to have the largest ones in the case of H3N2 IAV population. The results of suggest that provinces in the South of Ecuador may be acting as a source of Influenza while other provinces may act as a sink. Co-circulation of different genetic lineages was observed in both H1N1 pdm09 and H3N2
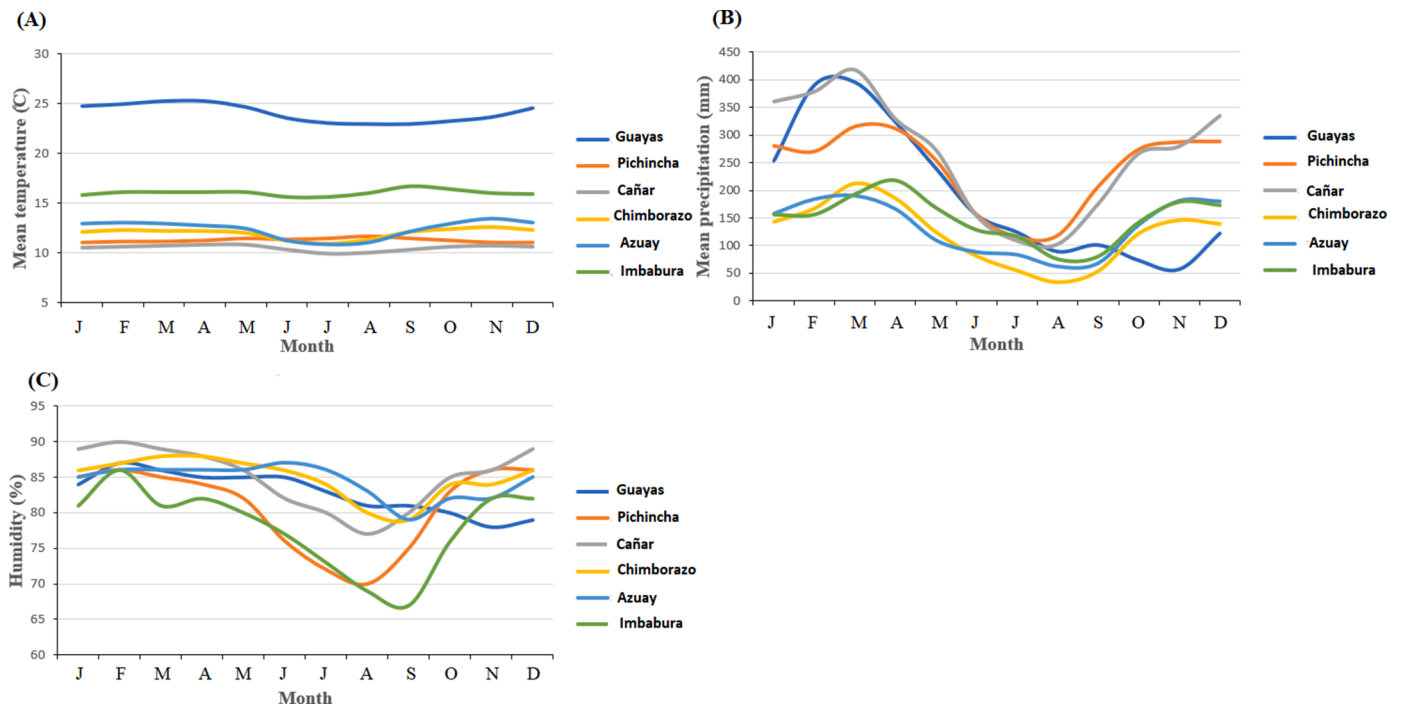
**(A)**



**(B)**



**(C)**



**Fig. 3.** Climatic parameters of Ecuadorian provinces. Mean monthly temperatures, precipitation and humidity in different Ecuadorian provinces are shown in A, B and C, respectively. Colors assigned to each province is indicated at the right of each graph.

**Table 2**
Bayesian coalescent inference of IAV isolated in Ecuador.

| Group[a] | HPD[c] | ESS[d] | Parameter | Value[b] |
|---|---|---|---|---|
| H1N1 HA complete sequences | | | Posterior | −3767.77 |
| −3796.46 to −3738.22 | 805.90 | | | |
| | | | Prior | −197.32 |
| | −232.00 to −160.60 | 623.10 | | |
| | | | Likelihood | −3570.44 |
| | −3592.56 to −3550.57 | 831.80 | | |
| | | | *Ne* Azuay[e] | 0.523 |
| | 0.025 to 1.516 | 2765.80 | | |
| | | | *Ne* Chimborazo | 0.197 |
| | $4.12 \times 10^{-3}$ to 0.745 | 983.30 | | |
| | | | *Ne* Guayas | 1.515 |
| | 0.067 to 4.466 | 2160.00 | | |
| | | | *Ne* Pichincha | 0.061 |
| | 0.014 to 0.121 | 1054.50 | | |
| | | | *Ne* Manabi | 0.826 |
| | $6.54 \times 10^{-3}$ to 3.395 | 1578.20 | | |
| | | | tMRCA[f] | 4.17 |
| | 4.00 to 4.36 | 2950.80 | | |
| | | | | **01/16/2016** |
| H3N2 HA complete sequences | | | Posterior | −3806.15 |
| −3830.48 to −3781.60 | 536.30 | | | |
| −273.89 to −217.38 | 755.50 | | Prior | −245.34 |
| −3577.91 to −3544.49 | 3959.60 | | Likelihood | −3560.81 |
| $3.91 \times 10^{-3}$ to 3.973 | 896.20 | | *Ne* Azuay | 1.130 |
| 0.010 to 4.675 | 2155.70 | | *Ne* Cañar | 1.430 |
| | | | *Ne* Chimborazo | 0.630 |
| 0.013 to 2.205 | 1434.30 | | *Ne* Guayas | 1.431 |
| 0.019 to 4.740 | 2077.90 | | *Ne* Pichincha | 0.557 |
| 0.020 to 2.304 | 346.40 | | | |
| | | | tMRCA[f] | 4.817 |
| | 4.393 to 5.245 | | | |
| | 6442.20 | | | |
| | | | | **01/23/2016** |

[a] See Supplementary Material Table 1 for strains included in this analysis. [b]In all cases, the mean values are shown. [c]HPD, high probability density values. [d]ESS, effective sample size. [e]*Ne*, effective population size. [f]tMRCA, time of the most common recent ancestor is shown in years. The date estimated for the tMRCA is indicated in bold.

IAV isolated in Ecuador. These results revealed that different genetic lineages co-circulate in different geographic regions of Ecuador at the same time.

**Interest**

Montevideo, January 20th, 2023.
Dr. Esteban Domingo
Editor
Virus Research
Dear Dr. Domingo:
The reason of this letter is to let you know that Alfredo Bruno, Natalia Goñi and Juan Cristina, we are the authors of the manuscript "Spatial, temporal and evolutionary insight into seasonal epidemic Influenza A virus strains near the equatorial line: the case of Ecuador".

All authors do not have any conflict of interest and we do not have any interest to declare.

All authors have read and approved the final version of this manuscript.

Sincerely,
Dr. Juan Cristina
Corresponding author
Dr. Juan Cristina
Corresponding author

**CRediT authorship contribution statement**

**Alfredo Bruno:** Resources, Data curation, Visualization, Investigation. **Natalia Goñi:** Writing – review & editing. **Juan Cristina:** Conceptualization, Methodology, Writing – original draft.
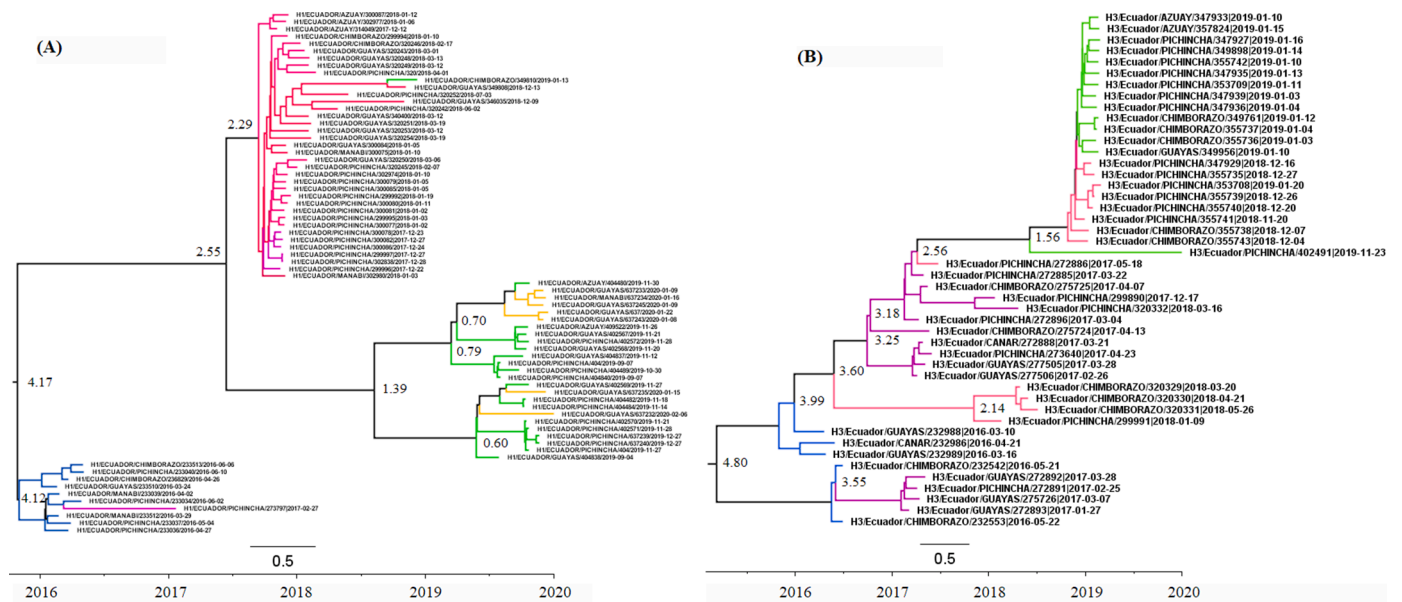
**Fig. 4.** Bayesian MCMC phylogenetic tree analysis of IAV strains circulating in Ecuador. Maximum clade credibility trees obtained using the HKY+γ nucleotide model, a relaxed molecular clock and a structured coalescent method using MASCOT are shown. The trees are rooted to the Most Recent Common Ancestor (MRCA). Time to the MRCA is shown in years at the bottom of the figure. Bar at the bottom of the trees denote time in years. Numbers next to the branches show the median height of the branch. Strains in the tree are indicated by type and name followed by date of isolation. Nodes are colored according to the year of isolation. The results found for H1N1 and H3N2 strains are shown in (A) and (B), respectively.

## Declaration of Competing Interest

The authors declare that they have no known competing financial interests or personal relationships that could have appeared to influence the work reported in this paper.

## Data availability

Data will be made available on request.

## Supplementary materials

Supplementary material associated with this article can be found, in the online version, at doi:10.1016/j.virusres.2023.199051.

## References

Alonso, W.J., McCormick, B.J., 2012. EPIPOI: a user-friendly analytical tool for the extraction and visualization of temporal parameters from epidemiological time series. BMC Public Health 982. https://doi.org/10.1186/1471-2458-12-982, 12.

Alonso, W.J., Yu, C., Viboud, C., et al., 2015. A global map of hemispheric Influenza vaccinerecommendations based on localpatterns of viral circulation. Sci. Rep. 5, 17214. https://doi.org/10.1038/srep17214.

Azziz, A., Baumgartner, E., Dao, C., Nasreen, S., Uddin, M., Mah-E-Munner, S., et al., 2012. Seasonality, timing, and climate drivers of Influenza activity worldwide. JID 206. https://doi.org/10.1093/infdis/jis467.

Bouckaert, R., Vaughan, T.G., Barido-Sottani, J., Duchene, S., Fourment, M., Gavryushkina, A., et al., 2019. BEAST 2.5: an advanced software platform for Bayesian evolutionary analysis. PLoSComput. Biol. 15, e1006650 https://doi.org/10.1371/journal.pcbi.1006650.

Ferguson, N.M., Galvani, A.P., Bush, R.M., 2003. Ecological and immunological determinants of Influenza evolution. Nature 422, 428–433. https://doi.org/10.1038/nature01509.

Hirve, S., Newman, L.P., Paget, J., et al., 2016. Influenza seasonality in thetropics and subtropics–when to vaccinate? PLoS One 11, e0153003. https://doi.org/10.1371/journal.pone.0153003, 2016.

Lemey, P., Rambaut, A., Bedford, T., 2014. Unifying viral genetics and human transportation data to predict the global transmission dynamics of human Influenza H3N2. PLoS Pathog. 10, e1003932 https://doi.org/10.1371/journal.ppat.1003932.

Neumann, G., Brownlee, G.G., Fodor, E., Kawaoka, Y., 2004. Orthomyxovirus replication, transcription, and polyadenylation. Curr. Top. Microbiol. Immunol. 283, 121–143. https://doi.org/10.1007/978-3-662-06099-5_4.

De Mello, W.A., De Paiva, T.M., Ishida, M.A., et al., 2009. The dilemma of Influenza vaccine recommendations when applied to the tropics: the Brazilian case examined under alternative scenarios. PLoS One 4, e5095. https://doi.org/10.1371/journal.pone.0005095.

Müller, N.F., Rasmussen, D., Stadler, T., 2018. MASCOT: parameter and state inference under the marginal structured coalescent approximation. Bioinformatics. https://doi.org/10.1093/bioinformatics/bty406 bty406.

N'gattia, A.K., Coulibaly, D., Nzussouo, N.T., Kadjo, H.A., Chérif, D., Traoé, Y., Kouakou, B.K., Kouassi, P.D., Ekra, K.D., Dagnan, N.S., Williams, T., Tiembré, I. 2016. Effects of climatological parameters in modeling and forecasting seasonal influenza transmission in Abidjan, Cote d'Ivoire. BMC Public Health. 16, 972. doi: 10.1186/s12889-016-3503-1.

Katoh, K., Rozewicki, J., Yamada, K.D., 2019. MAFFT online service: multiple sequencealignment, interactive sequence choice and visualization. Brief. Bioinform. 4, 1160. https://doi.org/10.1093/bib/bbx108.

Kitler, M.E., Gavinio, P., Lavanchy, D., 2002. Influenza and the work of the World Health Organization. Vaccine 20, S5–S14. https://doi.org/10.1016/S0264-410X(02)00121-4.

Richard, S.A., Viboud, C., Miller, M.A., 2010. Evaluation of southern hemisphere Influenza vaccine recommendations. Vaccine 28, 2693–2699. https://doi.org/10.1016/j.vaccine.2010.01.053.

Scalera, N.M., Mossad, S.B., 2009. The first pandemic of the 21st century: a review of the 2009 pandemic variant Influenza A (H1N1) virus. Postgrad. Med. 121, 43–47. https://doi.org/10.3810/pgm.2009.09.2051.

Scholtissek, C., Von Hoyningen, V., Rott, R., 1978. Genetic relatedness between the new 1977 epidemic strains (H1N1) of Influenza and human Influenza strains isolated between 1947 and 1957 (H1N1). Virology 89, 613–617. https://doi.org/10.1016/0042-6822(78)90203-9.

Soebiyanto, R.P., Clara, W., Jara, J., et al., 2014. The role of temperature and humidity on seasonal Influenza in tropical areas: guatemala, El Salvador and Panama, 2008–2013. PLoS One 9, e100659. https://doi.org/10.1371/journal.pone.0100659.

Suntronwong, N., Vichaiwattana, P., Klinfueng, S., et al., 2020. Climate factors influence seasonal Influenza activity in Bangkok,Thailand. PLoS One 15, e0239729. https://doi.org/10.1371/journal.pone.0239729.

Tamerius, J.D., Shaman, J., Alonso, W.J., Bloom-Feshbach, K., Uejio, C.K., Comrie, A., Viboud, C., 2013. Environmental predictors of seasonal Influenza epidemics across temperate and tropical climates. PLoS Pathog. 9 (3), e1003194 https://doi.org/10.1371/journal.ppat.1003194.

Trifinopoulos, J., Nguyen, L.T., Von Haeseler, A., Minh, B.Q., 2016. W-IQ-TREE: a fast online phylogenetic tool for maximum likelihood analysis. Nucleic Acids Res. 44 (W1), W232–W235. https://doi.org/10.1093/nar/gkw256.

Viboud, C., Alonso, W.J., Simonsen, L., 2006. Influenza in tropical regions. PLoS Med. 3, 468–471. https://doi.org/10.1371/journal.pmed.0030089.

Wessa, P.. Free statistics software, Office of research development and education, version 1.2.1. https://www.wessa.net.

Wolf, Y.I., Viboud, C., Holmes, E.C., Koonin, E.V., Lipman, D.J., 2006. Long intervals of stasis punctuated by bursts of positive selection in the seasonal evolution of Influenza A virus. Biol. Direct 1, 34. https://doi.org/10.1186/1745-6150-1-34.